Wetting Angles on Illuminated Ta_2O_5 Thin Films with Controlled Nanostructure

Victor Rico,[†] Ana Borrás,[†,‡] Francisco Yubero,[†] Juan P. Espinós,[‡] Fabián Frutos,[§] and Agustín R. González-Elipe*[,†]

Laboratorio de Superficies y láminas delgadas, Instituto de Ciencia de Materiales de Sevilla (CSIC-Universidad de Sevilla), Avenida Américo Vespucio 49, 41092 Sevilla, Spain, EMPA, Swiss Federal Laboratories for Materials Testing and Research, Feuerwerkerstrasse 39, 3604, Thun, Switzerland, and Departamento de Física Aplicada I, Universidad de Sevilla, Avenida Reina Mercedes s/n, 41012 Sevilla, Spain

Ta_2O_5 thin films with different nanostructure and surface roughness have been prepared by electron evaporation at different angles between the evaporation source and the substrates. Large variation of refraction indexes (n) from 1.40 to 1.80 were obtained by changing the geometry of evaporation and/or by annealing the evaporated films at increasing temperatures up to 1000 °C to make them crystalline. Very flat and compact thin films ($n = 2.02$) were also obtained by assisting the growth by bombardment with O_2^+ ions of 800 eV kinetic energy. A similar correlation has been found between the wetting contact angle of water and the roughness of the films for the evaporated and evaporated + annealed samples, irrespective of their procedure of preparation and other microstructural characteristics. When the films were illuminated with UV light of $h > E_g = 4.2$ eV (E_g, band gap energy of Ta_2O_5), their surface became superhydrophilic (contact angle < 10°) in a way quite similar to those reported for illuminated TiO_2 thin films. The rate of transformation into the superhydrophilic state was smaller for the crystalline than for the amorphous films, suggesting that in Ta_2O_5 the size of crystal domains at the surface is an important parameter for the control of this kinetics. Changes in the water contact angle on films illuminated with visible light were also found when they were subjected to implantation with N_2^+ ions of 800 eV kinetic energy. The origin of this photoactivity is discussed in terms of the electronic band gap states associated with the nitrogen-implanted atoms. The possibility of preparing antireflective and self-cleaning coatings of Ta_2O_5 is discussed.

Introduction

The control of the wetting properties of materials (i.e., the contact angle of liquids on their surfaces) is a subject of much scientific interest with many practical and industrial implications.[1] Within this context, the discovery by Wang et al.[2] that the surface of TiO_2 may be transformed upon UV light irradiation from partially hydrophobic (i.e., water contact angles around 80°) into fully hydrophilic (i.e., the water drops spread on the surface), fostered the research on this material and this particular property.[3−6] At present, the use of TiO_2 as self-cleaning and an antifogging material is a reality that has been incorporated into some types of commercial glasses. Other applications such as automobile side view mirrors, window films, exterior tiles, and highway road wall panels, etc., have been also proposed.[7]

Despite the photoactive character of many other oxide semiconductors, the change in water contact angle upon light irradiation has only been extensively studied for TiO_2. Thus, although a similar behavior has been described for epitaxial layers of ZnO[8] or for thin films of semiconductor oxides such as ZnO, SnO_2, WO_3, and V_2O_5,[9] a systematic study of the UV-induced wetting angle changes on oxide semiconductors other than TiO_2 is still missing.

Another open issue for the practical implementation of these photoactive surfaces is to make them sensitive to photons in the visible region of the spectrum. Visible light activity for TiO_2 has been claimed by Asahi et al.,[10] when these films were doped with nitrogen. Recently, we have studied the wetting behavior upon UV and visible light irradiation of a series of oxide semiconductors in the form of thin films including ZnO, ITO commercial glass, Ta_2O_5, and $InTaO_4$.[11] In another recent work, we have also found that the modification of the outmost surface layers of TiO_2 by implantation of N_2^+ ions of 50 keV energy produces a change in the illumination response of the titanium oxide that becomes partially hydrophilic upon visible light irradiation.[12]

In the present work we want to go a step forward in the study of the wetting behavior of Ta_2O_5 thin films, trying to correlate their wetting response upon light irradiation with their optical properties and structural and microstructural characteristics. Parameters which have been considered for this investigation are the roughness of the films, their amorphous or crystalline character, or their surface modification by a beam of low-energy N_2^+ ions. Ta_2O_5 is a stable oxide with a band gap slightly larger and a refraction index smaller than those of TiO_2.[13,14] In addition to photocatalytic activity of this oxide in the form of powders when irradiated with UV[15] or visible[16,17] photons, this latter, when doped with nitrogen, has been also reported. These characteristics suggest that, under certain conditions, oxide layers of Ta_2O_5 might be an alternative to TiO_2 in the quest for photoactive thin films with self-cleaning properties. Indeed, this material, with a refraction index (n) smaller than that of TiO_2 would be a clear option when a coating with low n is a requisite (e.g., when looking for antireflective and self-cleaning coatings).[18]

* To whom correspondence should be addressed. E-mail: arge@icmse.csic.es.
† CSIC-Universidad de Sevilla.
‡ EMPA.
§ Departamento de Física Aplicada I, Universidad de Sevilla.

In the present work, amorphous Ta_2O_5 thin films with different nanostructures and porosities have been prepared by e-beam evaporation either at normal or glancing angle incidences.[19,20] In some cases annealing of the films at high temperature has been done to get the crystalline thin films. The comparative analysis of the optical properties and contact angle variation on the different thin films has provided some clues to assess the processes controlling the light-induced wetting transformation of this oxide in the form of thin film. An additional investigation with Ta_2O_5 thin films subjected to N_2^+ ion implantation has evidenced that this technique can be used to render their surface sensitive to visible light.

Experimental Section

T_2O_5 thin films were prepared by physical vapor evaporation (PVD) in an electron evaporation system. T_2O_5 pellets were used as material for evaporation. To get fully stoichiometric thin films, a constant oxygen partial pressure ($P \sim 10^{-4}$ torr) was maintained in the chamber during evaporation. The substrates, consisting of pieces of a silicon wafer or transparent silica plates, were kept at room temperature during the preparation of the films. To control the porosity and the surface roughness of the films, evaporation was carried out at different glancing angles with respect to the evaporation source. This geometry leads to columnar microstructures with much porosity and high surface roughness.[19,20] All the samples considered here were prepared by evaporation for the same period of time under equivalent rate conditions with an approximate growing rate at normal incidence of 6 nm min^{-1}. This means that the thickness of the samples prepared at glancing angles was smaller than that of those prepared with the sample placed normal with respect to the electron gun.

Another set of films were prepared by e-beam evaporation while their growth was assisted by low-energy (800 eV) O_2^+ ion bombardment (ion beam assisted deposition, IBAD[21]) and a beam current of 10 μA cm^{-2} (approximately an ion/atom ratio of 0.1). Some experiments were also carried out with thin films prepared at normal geometry that were subsequently subjected to 800 eV N_2^+ ion bombardment up to a dose of approximately 10^{17} ions cm^{-2}. The ion gun utilized in these experiments was a broad beam ion source (HFQ 1303-3 from Plasma Consult) supplied with N_2 and excited by a radio frequency (RF) discharge.

The as-prepared films were amorphous, but they could be made crystalline by postannealing in air at $t > 700$ °C for 3 h. Therefore, another set of samples used in this study consisted of thin films evaporated at normal geometry that were annealed in a furnace at increasing higher temperatures up to 1000 °C.

The crystalline structure of the annealed films was assessed by X-ray diffraction in a Siemens D5000 diffractometer working in the Bragg−Brentano configuration.

Illumination of the samples was carried out with a Xe lamp with a photon intensity at the position of the samples of 2 W cm^{-2} for the complete spectrum of the lamp. For simplicity we will refer to this situation in the text and figures as UV illumination. Other experiments consisted of the illumination with the same lamp by placing an UV filter between the lamp and the sample. The light intensity was then 1.6 W cm^{-2} at the sample position. In all cases an infrared filter (i.e., a water bath) was kept between the lamp and the samples to prevent any possible heating by the infrared radiation. From experiments with TiO_2 it is known that the wetting angle variation upon UV illumination is much affected by the temperature of the film and the external humidity.[22] In our case, we controlled the temperature of the holder during a complete illumination experiment and found that it did not change by more than 10 °C. All the experiments were carried out under similar conditions of the laboratory, and no significant variations in ambient humidity should be expected.

Measurement of contact angle was carried out by the Young method by dosing small droplets of deionized and bidistilled water on the surface of the illuminated samples. In the experiments where the contact angle variation was determined as a function of the illumination time, a metal foil acting as a shutter was used to close and open the lamp output. All wetting angle measurements within a given experiment were taken after illumination for successive periods of time. Therefore, the time scale in the plots refers to the accumulative illumination of the samples. The maximum uncertainty in the determination of the water contact angle is about 10°, depending on the sample position. In the course of this investigation it was noticed that the "as-prepared" thin films were more hydrophilic than the same samples a given time after their preparation. Therefore, storage conditions were carefully controlled by putting the samples in a desiccator until their use. The reported experiments were carried out with samples that have been stored for a sufficiently long period of time, so that they had stabilized their surface properties (the minimum time elapsed was 2 months since their preparation). The evolution of the wetting angles on the samples prepared at different glancing angles stored for increasing periods of time is presented in Supporting Information S1.

Chemical analysis of the original samples and the films subjected to N_2^+ ion bombardment has been carried out by means of X-ray photoemission spectroscopy (XPS) in a ESCALAB 210 spectrometer supplied by VG. The Mg Kα (i.e., 1253.6 eV) line was used as excitation source, and the spectra were collected in the pass energy constant mode at a value of 50 eV. Calibration of the binding energy (BE) scale was done by referencing the energy scale to the C1s peak at 284.6 eV for the adventitious carbon present on the surface of samples. Some of the samples containing nitrogen were also analyzed after sputtering with Ar^+ ions of 1000 eV kinetic energy. An erosion rate of approximately 1 nm min^{-1} was achieved under our experimental conditions. A treatment of ca. 5 min was considered sufficient to remove the most external surface layers of the films.

The optical properties of the samples were determined by UV−vis absorption spectroscopy on a Perkin-Elmer Lambda 12 spectrometer for samples prepared on fused silica and by spectroscopic ellipsometry for samples prepared on a silicon wafer. Typical thickness of the samples used for optical characterization was around 350 nm. By the UV−vis absorption experiments, the refraction index of the films was determined by simulating the oscillations appearing in the spectra of Ta_2O_5 thin films deposited on a substrate with a smaller refraction index. The spectroscopic ellipsometry experiments were performed using a Sopra commercially available system.

The measurements of ellipsometric parameters were made at wavelengths from 0.21 to 1.0 μm at 65, 70, and 75° angles of incidence. The analysis procedure consists of a regression using a Cauchy law to simulate the refraction index

$$n(\lambda) = \sqrt{1 + \frac{(n_\infty{}^2 - 1)\lambda^2}{\lambda^2 - \lambda_\infty{}^2}}$$

where λ is the wavelength, n the refractive index, $n_\infty$is the refractive index when $\lambda \rightarrow \infty$, and λ_∞ is the wavelength for

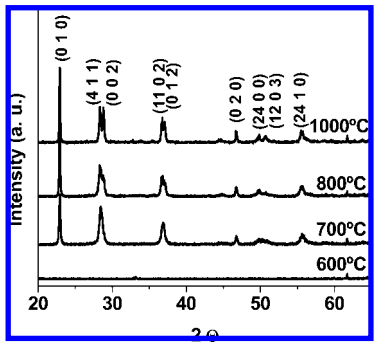

Figure 1. XRD spectra of the Ta_2O_5 thin films prepared at normal geometry of evaporation and subsequently annealed at increasing temperatures as indicated.

$n \rightarrow \infty$. To extract the extinction coefficient of the layer, we used the followoing expression:

$$K = K_0 + \left(\frac{K_1}{\lambda}\right)^3$$

The shape of the k vs λ curves was very similar in all cases. They were characterized by practically zero absorption in the visible region of the spectra and an absorption onset at about 4.1−4.2 eV typical of the bandgap of Ta_5O_5.

The reported values of refraction index measured by UV−vis or ellipsometry were determined at 550 nm. These two techniques yielded similar values of the refraction index, except for differences of the order of 0.01 in some determinations. These differences will not be considered for the discussion of the results. This good agreement supports that the microstructure of the films is similar on the two substrates, fused silica and silicon wafers, used to grow the films. Optical properties were not analyzed for the films annealed at $T > 700$ °C because the scattering of light distorted the UV−vis and ellipsometry spectra.

Normal and cross-section scanning electron micrographs were taken in a Hitachi S5200 field emission microscope working at 5.0 keV. For this analysis the samples were prepared on a silicon wafer substrate that was cleaved for observation of the layer cross-sections.

Atomic force microscopy (AFM) images of the surface of samples were taken with a Dulcinea microscope from Nanotec (Madrid, Spain) working in tapping mode and using high-frequency levers. AFM images were processed with the WSxM free available software from Nanotec. For each thin film, more than five good quality images were taken at different regions of the sample. The derived root mean square (rms) values were determined for a representative image of the surface and agree well with the average values of all images.

Results

Structure of Thin Films. Just after preparation by electron evaporation the thin films were amorphous, but they became crystalline after an annealing treatment in a furnace at $t>700$ °C, as indicated in the Experimental Section. Figure 1 shows a series of X-ray diffraction (XRD) diagrams corresponding to thin films that were grown by evaporation at normal geometry and then annealed at the indicated temperatures. These diagrams confirm that the thin films have become crystalline by annealing, depicting the hexagonal (at 700 °C) and orthorhombic (at 1000 °C) structure of Ta_2O_5.[23] The films present a preferential texturing according to the (003) and the (001) planes for respectively the hexagonal and orthorhombic structures. From the width of these peaks, the size of the crystal domains has been determined by the method of Sherrer. The obtained values are reported in Table 1, showing that the size of the crystal domains increases for the films annealed at 1000 °C.

TABLE 1: Summary of Main Properties of Ta_2O_5 Thin Films

sample	refraction index	rms (nm)	size of crystal domains (nm)	contact angle (deg)
normal evaporation	1.80	2	amorphous	97
evaporation 60°	1.59	2.7	amorphous	61
evaporation 70°	1.51	4	amorphous	58
evaporation 80°	1.37	14.5	amorphous	50
evaporation 85°	1.36	8.24	amorphous	51
evaporation 90°	1.47	11.3	amorphous	54
annealed 600 °C	1.80	2.50	amorphous	80
annealed 700 °C		2.80	58	73
annealed 800 °C		4.9	55	69
annealed 1000 °C		11.4	75	57
IBAD films	2.02	0.73	amorphous	96

Microstructure and Optical Properties of Thin Films. Figure 2 shows a series of scanning electron microscopy (SEM) cross-section-view micrographs corresponding to the Ta_2O_5 thin films prepared at normal evaporation and then annealed at increasing higher temperatures and by assisting their growth by O_2^+ ion bombardment. This treatment is expected to yield more compact and flat thin films.[21] It will be shown below that these samples present very little surface roughness and that, therefore, they can be considered as a good reference of an almost flat surface. Meanwhile, the annealed films present a microstructure where large grains separated by relatively big voids can be observed. The size of the grains and that of the voids increases with the temperature of annealing, thus supporting an extensive sintering of the grains constituting the microstructure of the films.

Figure 3 shows equivalent SEM micrographs taken for the films prepared by evaporation at glancing angles. They are characterized by a tilted columnar and open microstructure that is typical of thin films prepared by glancing evaporation.[19,20] These films were not subjected to any further treatment, and therefore the obtained microstructure results from the deposition method using a glancing angle geometry. The angles formed between the columns and the substrate adjust well to those expected for this type of thin films depending on the geometry of evaporation. However, it must be noted some bending of the columns as the thickness of the films increases. This indicates a change in the growing mechanism of the films and certain heterogeneity in depth. Since this microstructural change is a second-order effect for the investigated wetting properties, we will not discuss it in detail in this paper. In principle, besides an increase in the angle of the tilted columns, the films prepared at more glancing geometries are expected to have a higher porosity. Transmission spectra recorded for the different studied samples are shown in Figure 4. They have been vertically displaced to clearly differentiate between the different curves. The films annealed at $T > 700$ °C depict a spectral shape typical of thin films that scatter the light. Therefore, the refraction index of these films could not be determined either by UV−vis absorption spectrometry or by ellipsometry. This behavior agrees with the large size of the crystal domains derived from the XRD diagrams and with the cross-section images of these films where large particles and big pores are clearly noticeable. From this series of samples, only the films annealed at 700 °C and the sample prepared by IBAD presented the typical shape of nondispersive transparent materials. The value of the refraction

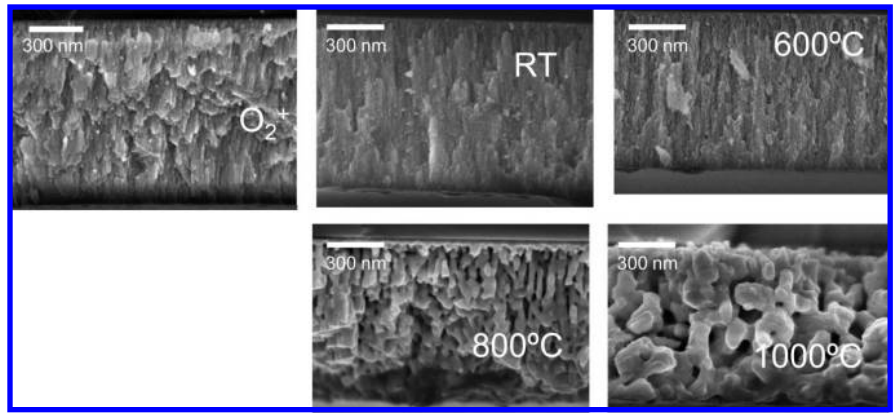

Figure 2. Cross-section SEM micrographs of the Ta_2O_5 thin films prepared at normal geometry of evaporation and subjected to annealing at increasingly higher temperatures as indicated.

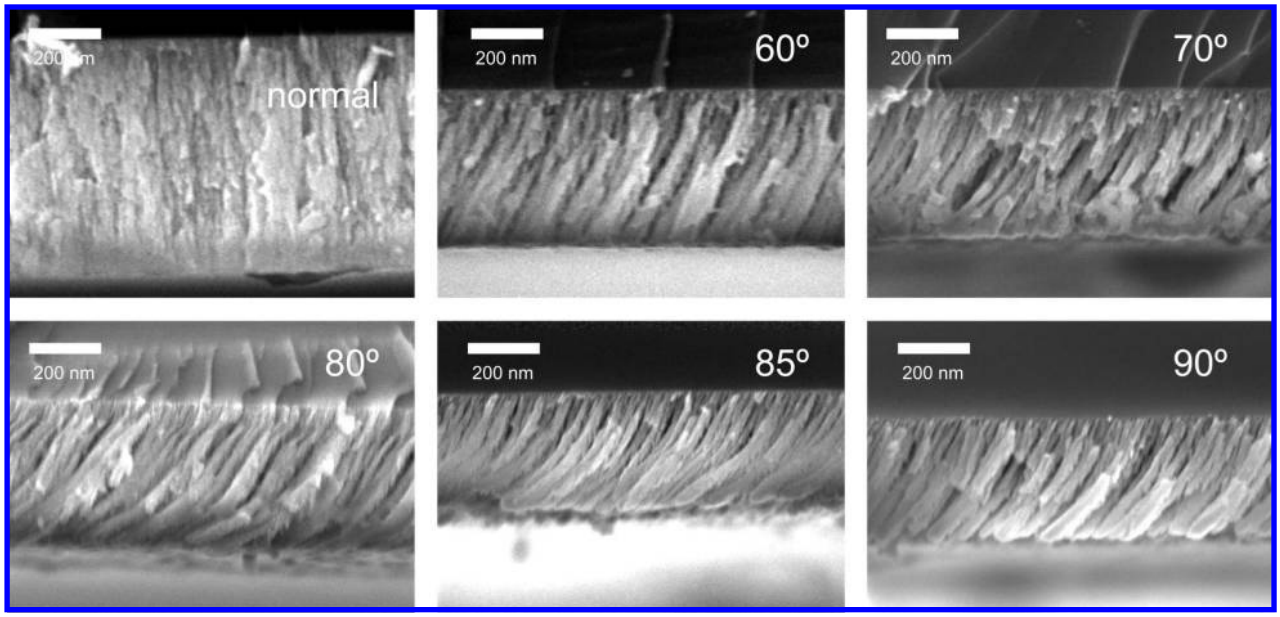

Figure 3. Cross-section SEM micrographs of the Ta_2O_5 thin films prepared by evaporation at different glancing angles as indicated.

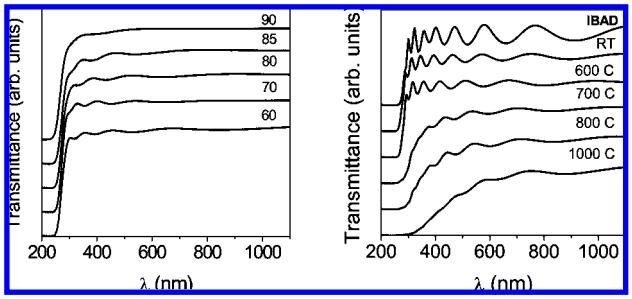

Figure 4. UV−vis transmission spectra of Ta_2O_5 thin films prepared by electron evaporation. (Left) Thin films prepared at different glancing angles as indicated. (Right) Thin films prepared at normal geometry and then subjected to annealing at the indicated temperatures as indicated. The spectrum of an IBAD thin film is also included.

indices (n) and band gap energies (E_g) were deduced from the analysis of these UV−vis absorption spectra or by ellipsometry and are summarized in Table 1.

The films prepared at glancing geometry of evaporation presented a well-defined spectral shape with oscillations that present very low amplitude. This indicates that these thin films have a refraction index that is very similar to that of the silica substrate. The different n values determined for these samples are also summarized in Table 1. It is apparent in this table the large variations in n values found for these films that decrease with the evaporation angle (with the exception of the samples prepared at 90°). Refraction indices of thin films can be taken as an indirect measurement of their porosity.[24] Therefore, the obtained n values confirm that the porosity of the films increases for more glancing geometries of evaporation. It is interesting that the E_g values calculated for all the films by extrapolating to zero absorption the plot of $(\alpha E^{0.5})$ vs λ fit within a common similar value around 4.1−4.2 eV, in good agreement with the previously reported value of band gap for thin films of this material.[14]

Refraction indices ranging from 2.02 for the film prepared by assisting its growth with O_2^+ to 1.36 for the films prepared at an evaporation angle of 85° are obtained. The smallest n values of the films are similar to the n value of the silica substrate (i.e., around 1.45), and therefore the Ta_2O_5 prepared at evaporation angles higher than 85° behaves as antireflective coatings. This behavior is confirmed by the absence of oscillations in the experimental transmission spectra of these samples as reported in Figure 4.

Surface Roughness and Wetting Angles. A very important characteristic of the surfaces when dealing with their wetting properties is their roughness. According to the classical models of Wenzel,[25] Cassie,[26] or Miwa,[27] the actual contact angle on a

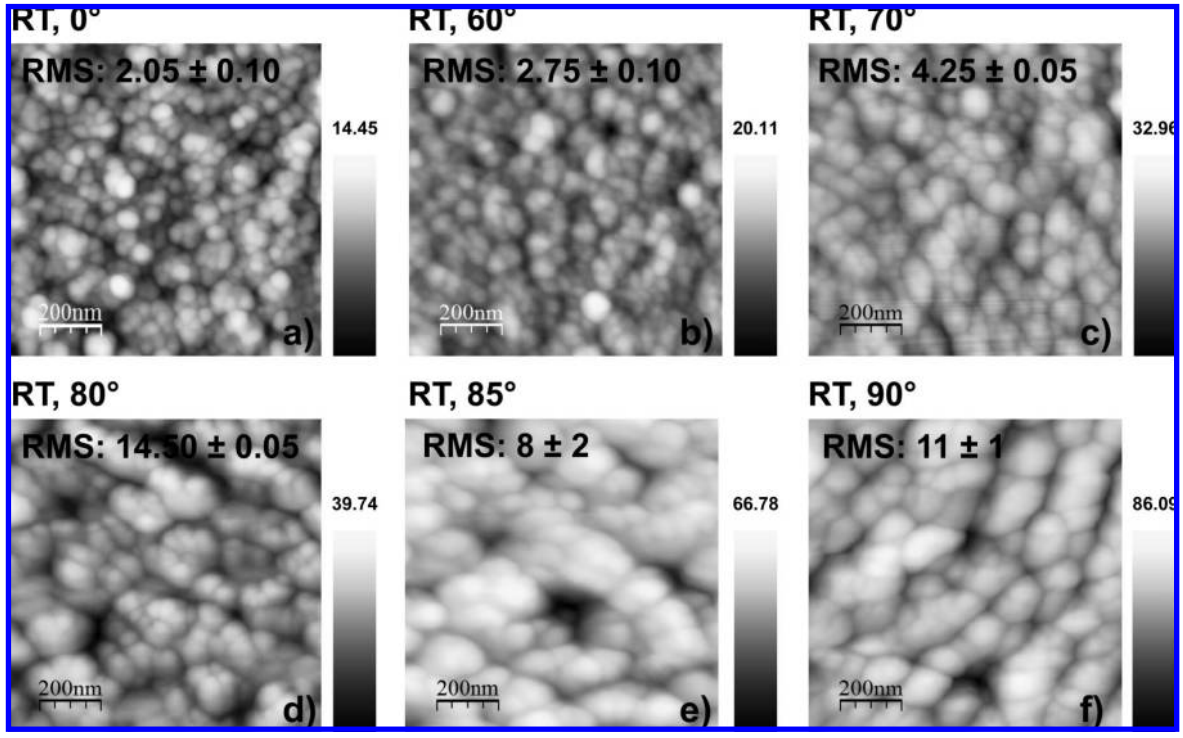

Figure 5. AFM images of the Ta_2O_5 thin films prepared by evaporation at different glancing angles as indicated.

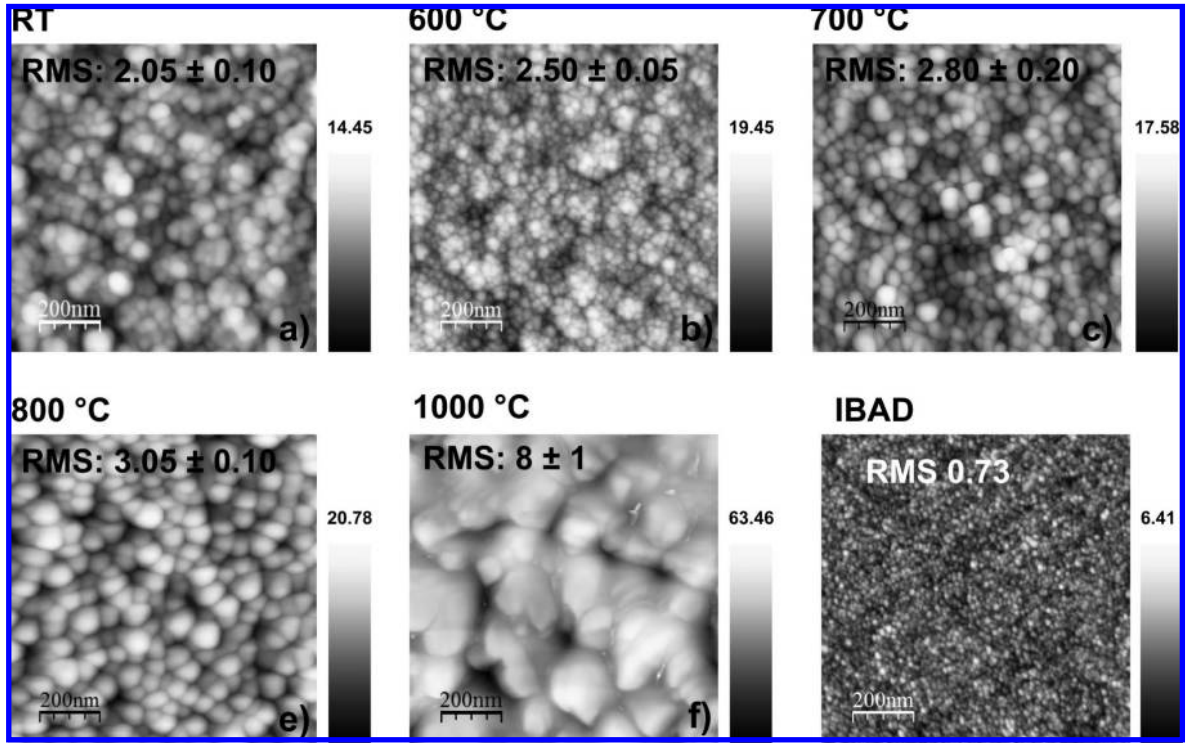

Figure 6. AFM images of the Ta_2O_5 thin films prepared at normal geometry of evaporation and subjected to annealing at increasing higher temperatures as indicated. The image of the IBAD sample is also included.

surface depends of its roughness. The proposed dependence on the roughness is different for each model. In principle, significant differences in surface roughness are to be expected for our samples due to the quite distinct microstructures found by SEM analysis of the different thin films. The AFM images of samples prepared at different glancing angles reported in Figure 5 clearly evidence that the surface is rougher as the evaporation angle increases (i.e., see the gray scale included in the figure). Meanwhile, the AFM of the annealed samples reported in Figure 6 shows that their roughnesses increase with the annealing temperature. In this figure, it is also apparent that the thin film prepared by assisting its growth by ion bombardment depicts a very flat surface. This is actually the behavior expected for IBAD films,[21] a sample that is included in the present set of experiments as a reference of an almost flat sample. A quantitative evaluation of the roughness is provided by the rms values. A compilation of these values is reported in Table 1. It is apparent in this table that for the two series of samples the

TABLE 2: Rate Constant for the Evolution of the Cosine of Wetting Angles under Illumination and in the Dark for Samples Annealed at Increasing Temperatures

annealing temperature (°C)	grain size (nm)	K(UV) (min^{-1})	K(dark) (min^{-1})
25	7.5	1.18	-3.89×10^{-1}
600	8.6	4.35×10^{-1}	-1.49×10^{-1}
700	10.7	3.40×10^{-1}	-5.40×10^{-2}
800	11.6	2.42×10^{-1}	-2.62×10^{-2}
1000	41.2	9.0×10^{-2}	-4.26×10^{-3}

obtained rms values are within the same order of magnitude, varying from 0.73 for the IBAD thin film to 14.5 for the sample prepared at a glancing angle of 80°. At this point it is important to remark that, according to Tables 1, samples prepared at 85 or 90° glancing angles are neither the more porous nor the rougher from this series of samples prepared at glancing evaporation. The fact that the tilted columns forming the microstructure of these samples bend at a given thickness for samples prepared at glancing angles higher than 80° indicates that the growing mechanism is changing and deviating from the general predictions of the models developed to account for the growth of this type of films.[19,20] However, for the purposes of the present work, the most important point is that we have prepared two series of samples that, except for the IBAD film, display rms values within the same range.

For the two sets of samples we have checked the dependence of the wetting angle on this thin film characteristic. The contact angle measured on the thin films prepared by electron evaporation depended on both the roughness of the films and on the time elapsed since their preparation. This latter dependence is illustrated in Supporting Information S1. The annealed films did not show any aging process leading to a change in the wetting angle. However, the wetting angle for the two series of films did show a strong dependence on the roughness of the films. Figure 7 represents the values of wetting contact angles against the rms values for the series of annealed and IBAD films and for the set of evaporated samples in their steady state. It is worth noting that the two curves depict a similar profile.

Wetting Angle and Effect of the UV Illumination. Since Ta_2O_5 is a photoactive oxide semiconductor when irradiated with photons with sufficiently high energy (i.e., $E > E_g$),[16,28] it can be expected that, in a similar way than for TiO_2, its surface becomes superhydrophilic (i.e., wetting angle smaller than 10°). In a previous publication we have presented a preliminary analysis of this effect for Ta_2O_5 thin films prepared by electron evaporation at normal geometry.[11] Figure 8 shows the evolution

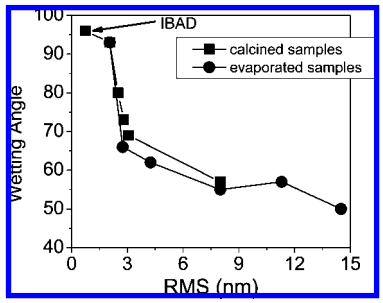

Figure 7. Representation of the wetting angles as a function of the roughness of the films expressed in terms of their rms for the Ta_2O_5 thin films prepared at glancing angles of evaporation or annealed at increasing temperatures. A point corresponding to the IBAD sample is also included.

of the contact angle as a function of the illumination time with UV photons to reach the superhydrophilic state (i.e., wetting angles smaller than 10°) and the posterior evolution of this contact angle when the samples were kept in the dark. For clarity, only the response behavior of some selected samples from the two series of thin films are represented in this figure. It is important to stress that no change in contact angle could be observed if the Ta_2O_5 thin films were irradiated with photons of lower energy than their E_g or when they were directly exposed to the sun light. The films prepared by evaporation present a very fast response, becoming hydrophilic after a few seconds of UV light irradiation. Due to this fast response no clear differences could be detected between the different samples. By contrast, the annealed films presented a slower response and became superhydrophilic when they were irradiated for longer periods of times. For this series of films it is also possible to observe that the response time slows down with the annealing temperature. A similar tendency can be noticed for the kinetics of recovery in the dark which is slower for the samples annealed at high temperatures. It is also worth noting that for the nonannealed samples the recovery of the wetting angle is much slower for the samples prepared at glancing angles than for those prepared at a normal geometry of evaporation.

The kinetics of the evolution of the contact angle of illuminated TiO_2 thin films has been thoroughly studied by Sechi and Tachiya.[29] These authors found a clear dependence between the cosine of the wetting angle and both the illumination and the recovery time in dark. We have tried a similar analysis for the series of annealed films. Figure 9 shows as an example the evolution with time of the cosine of the contact angles for the Ta_2O_5 thin film prepared by evaporation at normal geometry and for this film annealed at 1000 °C. This figure also depicts two dashed curves corresponding to fitting exponentials of the type $\exp(Kt)$ that reproduce the experimental curves. For simplicity we have assumed that there is just one single process (one single curve) for either the contact angle decay during illumination or for its recovery in dark. Values for the exponential constants K found for the annealed samples are gathered in Table 2 for the complete set of annealed thin films. The absolute values of these constants decrease with the temperature of annealing. Trying to correlate the distinct evolution of contact angle with a morphological characteristic of the samples, we have included in Table 2 the mean size of the grains that constitute the surface topography of these samples as deduced from their AFM images in Figure 6. For the determination of this mean size we have used the so-called Bearing plots of the surface features (see Supporting Information S2). The gathered values evidence that there is a good correlation between the kinetic constants and the mean size of surface grains.

Illumination with Visible Light and Nitrogen Implantation. A critical point by the use of photoactive band gap oxide semiconductors is the quest for materials that react when illuminated with visible light. In a previous work, we showed that TiO_2 with implanted nitrogen ions becomes partially hydrophilic when illuminated with visible light.[12] In the present work we have checked the effect of implanting low-energy ions on the Ta_2O_5 amorphous thin film prepared by evaporation. Analysis by XPS (Figure 10) of the topmost surface layers of the implanted material show the appearance of a shoulder around 400 eV superimposed on the Ta4p photoemission peak of Ta_2O_5. This shoulder can be attributed to implanted nitrogen species.[10,12,30] Unfortunately, the fact that this peak appears superimposed on the tantalum peak precludes both an accurate quantification of

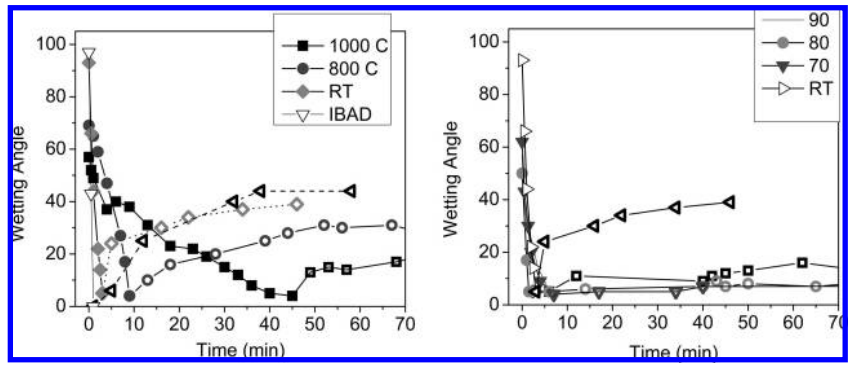

Figure 8. Evolution of the wetting angle for selected Ta_2O_5 thin films as a function of the UV irradiation time (closed symbols and open triangle symbols with a thin edge) and recovery of the wetting angle when the films are kept in the dark (open symbols with a thick edge). (Left) Samples subjected to annealing at increasing temperatures. (Right) Samples prepared by evaporation at glancing angles.

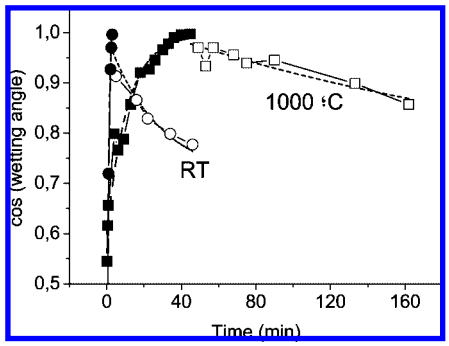

Figure 9. Evolution of the cosine of the contact angle for the sample prepared at normal evaporation and for this sample annealed at 1000 °C. Fitting curves are also included in the plot (see text).

the amount of implanted nitrogen on the topmost surface layers and a accurate determination of the BE of this peak. It is worth noting that the N1s peak disappears from the spectrum after prolonged Ar^+ sputtering of this sample, thus indicating that nitrogen is only distributed in the outermost layers of the films. Besides nitrogen, XPS also showed the appearance of a C1s peak typically attributed to contamination by the handling of the samples in air. This peak was used to define the BE scale in the spectra. Since both the intensity and shape of this peak were similar for the implanted and nonimplanted sample, we discard that this has an effective influence in the changes induced by illumination of the samples.

The effect of the illumination of this sample is reported in the experiment described in Figure 10. Here, it is apparent that illumination with visible light produces a slow but net decrease in the water contact angle from about 100 to about 60° in the steady state. A posterior illumination with UV light produces an additional and fast decrease in water contact angle up to reach the complete superhydrophilic state. By leaving the sample in the dark a slow recovery of the angle is thereafter found, in a way similar to the way it happens with the nonimplanted samples. It is important to remark that the implanted thin films presented a transparency similar to that of the nonimplanted films. This is due to the fact that the implantation zone is very thin, affecting to roughly 2.4 nm of the material according to SRIM calculations.[31]

Discussion

Structure, Microstructure, Surface Roughness, and Optical Properties of Ta_2O_5 Thin Films. The previous results have clearly evidenced that by changing the angle of deposition or by subjecting the thin films to high-temperature annealing, it is possible to control the microstructure and structure of Ta_2O_5 thin films prepared by electron evaporation. With this purpose, different conditions have been assayed including the evaporation at different glancing angles, the annealing of the films at increasing temperatures, or the use of O_2^+ beam bombardment. The wide set of n and rms values reported in Table 1 confirm that films with different compactness and surface roughness can be obtained by controlling the deposition conditions and the postdeposition treatments.

The films prepared at room temperature are amorphous, but they become crystalline by annealing at temperatures equal to or higher than 700 °C. The annealed films present different preferential texturing, size of crystalline domains, and surface roughness, these two latter parameters always increasing with temperature. The average size of the surface grains determined from the analysis of the AFM picture of the surface of samples also increases with the annealing temperature (see data in Table 2 and Supporting Information S2).

It is remarkable in Table 1 that the films prepared at very high evaporation angles present refraction indexes close or smaller to those of the quartz substrate. This means that these films may behave as antireflective coatings as it is shown by the fact that their absorption spectrum lies above that of the quartz substrate and presents no oscillations (cf. Figure 4 and Supporting Information S3). For solar collection devices and other related applications, the conjunction of a low refraction index and light-induced self-cleaning activity is of the outmost importance. This has been recently suggested as a way to increase the performance of Fresnel lenses and related concentration devices.[18]

Wetting Angle and Surface Topography of Ta_2O_5 Thin Films. Our study (cf. Figure 7) has shown that the wetting angle of the thin films is highly dependent on their roughness. As a general result, it is found that the wetting angle decreases with the roughness of the films expressed in terms of their rms values. However, the type of dependence cannot be well-described by a simple formula such as that proposed in the models by Wenzel[25] and others.[26,27] The main reason for that is that the nonannealed films prepared at normal evaporation or under IBAD conditions, characterized by the smallest rms values, present wetting angles higher than 90°, while the other films with higher rms values present wetting angles smaller than 90°. According to the assumptions of the aforementioned model, a rougher surface reinforces either the hydrophobic or the hydrophilic character of a flat sample of a given material. This means that the increase in roughness that we have found for the two series should reinforce the hydrophobic character of the IBAD or normal-evaporated samples, the opposite that we

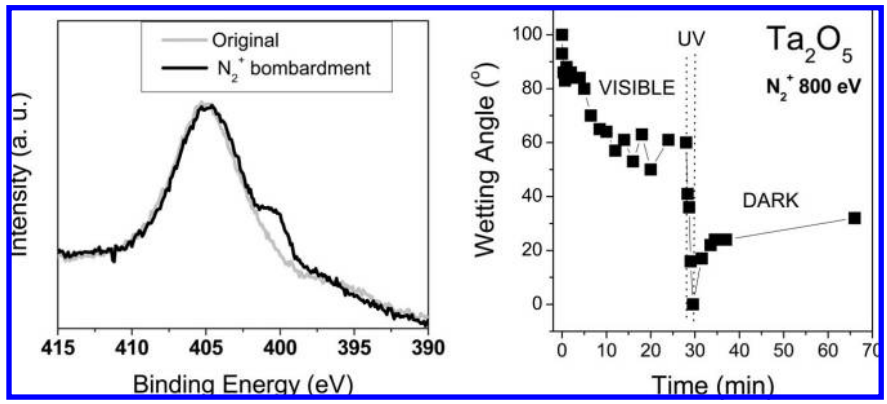

Figure 10. (Left) XPS spectrum of the N1s region showing a shoulder corresponding to this level superimposed on the much bigger Ta 4p peak for a Ta_2O_5 thin film prepared by evaporation at normal geometry and then bombarded with N_2^+ ions of 800 eV kinetic energy. An equivalent spectrum for an original Ta_2O_5 thin film before ion implantation is included for comparison. (Right) Evolution of the water contact angle on this thin film subjected first to visible and then UV + vis irradiation. The recovery of the wetting angle in the dark is also included.

have actually found (cf. Table 1). According to Yates et al.,[32] contamination of the surface of oxides by carbonaceous rests may produce an increase in contact angles. It is likely that such contamination occurs in our films because of their handling in air, thus leading to contact values higher than 90° for the normal evaporated and IBAD thin films (note that the measured values of these two thin films is close to 95°; cf. Figure 7). Effectively, XPS analysis of the surface of the sample showed a certain surface contamination by carbonaceous rests.

Thus, despite that all the contact angles of our samples cannot be reproduced by a simple model, the evolution of wetting angles reported in Figure 7 clearly indicates that, to a first approximation, the rms values determined by AFM is a parameter that directly control the contact angle of the Ta_2O_5 thin films kept in the dark. The fact that the annealed and nonannealed samples present a similar trend supports the use of this parameter to assess the dependence of roughness of contact angles of Ta_2O_5 thin films. At this point, it is also interesting to remark that, discarding the IBAD and normal evaporated samples, the Wenzel model[25] reproduces relatively well the evolution of the cosine of the wetting angles as a function of the roughness of the different thin films (see Supporting Information S4).

Wetting Angle on Illuminated Ta_2O_5 Thin Films. Wang et al.[2] explained the superhydrophilic transformation of the surface of irradiated TiO_2 by assuming that its surface becomes hydroxylated by the photocatalyzed dissociation of water molecules. A similar process can be proposed here to account for the transformation of the surface of the irradiated Ta_2O_5 thin films. Additionally, our results have shown that the transformation rate is different depending on the sample characteristics. Thus, all amorphous films depict very fast transformation kinetics into the superhydrophilic state, while the annealed and hence crystalline films transform with a slower kinetics. On the basis of this evidence, we can speculate that the transformation into the superhydrophilic state not only requires the light-induced hydroxylation of the surface but also implies the atomic rearrangement of the outermost surface layer of the films. This process would require surmounting a certain activation energy that would depend on the degree of atomic order at the surface and, for the crystalline films, on the size of the crystal planes exposed at the surface. In amorphous films, such a process would not require much activation energy and the transformation kinetic would be fast irrespective of the size of surface features. By contrast, for the crystalline films the transformation kinetics would slow down as the size and order of crystal planes at the surface increases. This is in fact supported by the comparison in Table 2 of the values of the kinetic constants and the size of the surface features determined by AFM. It must be stressed that this latter parameter is not a measurement of the size of crystal planes exposed at the surface, although its increase in size with the annealing temperature is a hint that the size of crystal planes also increases with this parameter. It is also worth noting that a similar correlation with the average size of the surface domains also exists for the kinetics of recovery of the wetting angle (cf. Figure 8 and Table 2). This correlation further supports that both processes, the transformation of the surface either into superhydrophilic or back to its original state before illumination, involve a collective response of the surface requiring of some activation energy.

N_2^+ Ion Implantation and Activation of Ta_2O_5 with Visible Light. One of the motivations of the present work is the quest for self-cleaning materials other than TiO_2 that can possess a double functionality, i.e., that their surface becomes hydrophihlic upon light irradiation and that they can be processed in the form of thin films with a low refraction index. These two features have been clearly demonstrated in Figures 4 and 8 for the Ta_2O_5 thin films prepared at glancing evaporation angles. According to the data reported in these figures and in Table 1, these films may act as antireflective coatings while simultaneously they become superhydrophilic under UV illumination. However, a clear limitation for the practical use of these coatings under solar light irradiation is that their band gap is larger than the UV photons of solar light.

Ta_2O_5 is an oxide semiconductor with a band gap of the order of 4.1−4.2 eV [13,14] This means that any photoactivated process has to be induced with photons with an energy higher than this value. We verified this requirement by proving that no change in water contact angle was induced when the Ta_2O_5 thin films are illuminated with photons with $h\nu < 4$ eV or with solar light. However, a change by more than 40° in contact angle was induced with visible light if N_2^+ ions of 800 eV are implanted in the Ta_2O_5 thin films (cf. Figure 9). This result is similar to that recently reported for TiO_2 thin films that were ion-implanted with N^+ ions of 50 keV kinetic energy.[12] The main difference between the two experiments is the energy of the ions and, therefore, the different penetration depth expected in each case. According to SRIM simulations carried out for these two experimental conditions,[31] approximate penetration depths of 2.4 and 93 nm are expected for, respectively, the implantation on Ta_2O_5 carried out here and the previous experiments with TiO_2. According to the existing theoretical models for N-doping

of TiO_2,[33,34] it must be expected that electronic levels in the band gap region are produced as a result of the ion implantation experiments. According to the classical theories of photocatalysis with wide oxide semiconductors,[35,36] electronic excitations from these states into the conduction band of Ta_2O_5 would be responsible for the observed photoactivity with visible photons. The fact that the illumination does not produce a complete superhydrophilic state (i.e., contact angle $< 10°$) as it happens with UV photons has been previously discussed by us for the implanted TiO_2 thin films.[12] In that case, we assumed that only a given type of surface species are energetically able to react with the photoholes created by excitation of the gap states. Since the superhydrophilic transformation would also require the reaction of other types surface species which are more energy-demanding, only photoholes created in the valence band (i.e., requiring UV light of sufficiently high energy) would be able to induce the complete transformation. Within this scheme, the fact that a similar situation is found here with doped Ta_2O_5 with a very shallow depth distribution of nitrogen species points to that the partial decrease in wetting angle under visible light irradiation is a superficial process that not necessarily involves the migration of photoholes from the bulk to the surface. Evidence supporting that the conventional UV-induced superhydrophilicity and the visible-induced hydrophilicity reported in Figure 10 are not equivalent processes is the fact that the rate of transformation with visible photons is much slower than with UV photons. The migration of photoholes through the Schottky barrier formed in the depletion layer of charge of oxide semiconductors is a requirement for the separation of photogenerated electrons and holes and, therefore, a requisite for the classical photoactivity of oxide semiconductors.[35,36] Apparently, this barrier is not a requisite for the contact angle changes induced with visible light in the implanted Ta_2O_5 thin films as the thickness of the implanted layer (i.e., 2.4 nm) is much thinner than the usual thickness of the depletion layer in oxide semiconductors (i.e., of the order of a few hundreds of nanometers).

Conclusions

The previous results and conclusions have shown that it is possible to prepare Ta_2O_5 thin films with quite different microstructures, textures, and optical properties. Preparation strategies based on the evaporation at glancing angles, ion bombardment and annealing at increasing higher temperatures have been essayed for this purpose. In this way, antireflective films with refraction indices equal to or even slightly smaller than that of quartz or glass have been prepared. The contact angles measured on the different thin films show a direct dependence on the surface roughness of the films, decreasing as the roughness, expressed in terms of rms values, increases.

When the Ta_2O_5 thin films are illuminated with photons with a $h \gg 4$ eV, the surface of the films become superhydrophilic (i.e., contact angle smaller than 10°). We claim that the combination of a low refraction index for the films (i.e., antireflective coatings) together with the self-cleaning activity derived from their superhydrophilicity might be a very positive combination of properties for certain applications in the field of solar collection.[18] A drawback for this application is the fact that very energetic photons are required to induce the transformation into the superhydrophilic state and that, therefore, solar light would be unable to induce such a change. However, changes in the wetting angles on Ta_2O_5 can be activated if thin films of this material are implanted with N_2^+ ions of low energy. Since this implantation, affecting just the few external layers of the films, does not significantly affect their transparency (i.e., from an optical point of view these films behave as pure Ta_2O_5 thin films and therefore do not appreciably filter the UV and near UV photons), we believe that this result is a first step in the development of antireflective coatings of this material that present self-cleaning activity when irradiated with visible light.

Acknowledgment. We acknowledge the financial contribution of the Spanish Ministry of Science and Technology (Projects MAT-2007-65764 and NAN2004-09317-C04-01 and CONSOLIDER-INGENIO 2010-CSD2008-00023), the Junta de Andalucía (Project TEP2275), and the European Union through its 6th framework program (Project NATAMA Project NMP3-CT-2006-032583). The support of the "Fundación Domingo Martínez" made possible the updating of the electron evaporation apparatus used for the preparation of the films.

Supporting Information Available: (S1) Plot of wetting angles as a function of surface roughness, (S2) Bearing plots from AFM images of the annealed Ta_2O_5 thin films, (S3) UV-vis transmission spectra of quartz plate and studied substrate, and (S4) text describing model for calculating r_W, applicable references, and figure showing the measured wetting angle compared to the r_W values. This information is available free of charge via the Internet at http://pubs.acs.org.

References and Notes

(1) Blossey, R. *Nat. Mater.* **2003**, *2*, 301.
(2) Wang, R.; Hashimoto, K.; Fujishima, A.; Chikuni, M.; Kojima, E.; Kitamura, A.; Shimohigoshi, M.; Watanabe, T. *Nature* **1997**, *388*, 431–431.
(3) Nakajima, A.; Hashimoto, K.; Watanabe, T. *Montash. Chem.* **2001**, *132*, 31–31.
(4) Stevens, N.; Priest, C. I.; Sedev, R.; Ralston, J. *Langmuir* **2003**, *19*, 3272–3272.
(5) Sakai, N.; Fujishima, A.; Watanabe, T.; Hashimoto, K. *J. Phys. Chem. B* **2001**, *105*, 3023.
(6) Miyauchi, M.; Kieda, N.; Hishita, Sh.; Mitsuhashi, T.; Nakajima, A.; Watanabe, T.; Hashimoto, K. *Surf. Sci.* **2002**, *511*, 401.
(7) Fujishima, A.; Hashimoto, K.; Watanabe, T. *TiO2 Photocatalyst, Fundamentals and Applications*; BKC: Tokyo, 1999.
(8) Miyauchi, M.; Shimai, A.; Tsuru, Y. *J. Phys. Chem. B* **2005**, *27*, 13307.
(9) Miyauchi, M.; Nakajima, A.; Watanabe, T.; Hashimoto, K. *Chem. Mater.* **2002**, *14*, 2812.
(10) Asahi, R.; Morikawa, T.; Ohwaki, T.; Aoki, K.; Taga, Y. *Science* **2001**, *293* (5528), 269.
(11) Rico, V.; López, C.; Borrás, A.; Espinós, J. P.; González-Elipe, A. R. *Solar Energy Mater. Solar Cells* **2006**, *90*, 2944.
(12) Borrás, A.; López, C.; Rico, V.; Gracia, F.; González-Elipe, A. R.; Richter, E.; Battiston, G.; Gerbasi, R.; McSporran, N.; Suthier, G.; György, E.; Figueras, A. *J. Phys. Chem. C* **2007**, *111*, 1801.
(13) Albella, J. M.; Martinez-Duart, J. M.; Rueda, F. *Opt. Acta* **1975**, *22*, 973.
(14) Babeva, T.; Atanassova, E.; Koprinarova, J. *Phys. Status Solidi A* **2005**, *202*, 330.
(15) Sayama, K.; Arawaka, H. *J. Photochem. Photobiol., A* **1994**, *77*, 243.
(16) Murase, T.; Irie, H.; Hashimoto, K. *J. Phys. Chem. B* **2004**, *108*, 15803.
(17) Hitoki, G.; Takata, T.; Hondo, J. N.; Hara, M.; Kobayashi, H.; Domen, K. *Chem. Commun. (Cambridge).* **2002**, *16*, 1698.
(18) Xi, Q.; Schubert, M. F.; Kim, J. K.; Schubert, E. F.; Chen, M.; Lin, S.-Y.; Liu, W.; Smart, J. A. *Nat. Photonics* **2007**, *1*, 176.
(19) van Popta, A. C.; Cheng, J.; Sit, J. C.; Brett, M. J. *J. Appl. Phys.* **2007**, *102*, 013517.
(20) Hawkeye, M. M.; Brett, M. J. *J. Vac. Sci. Technol., A* **2007**, *25*, 1317.
(21) González-Elipe, A. R. Yubero, F. Sanz, J. M. *Low Energy Ion Assisted Film Growth*; Imperial Collage Press: London, 2003.
(22) Takeuchi, M.; Sakamoto, K.; Martra, G.; Coluccia, S.; Anpo, M. *J. Phys. Chem. B* **2005**, *109*, 15422.
(23) Hummel, H. U.; Fackler, R.; Remmert, P. *Chem. Ber.* **1992**, *125*, 551.

(24) Mergel, D.; Buschendorf, D.; Eggert, S.; Grammes, R.; Samset, B. *Thin Solid Films* **2000**, *371*, 218.
(25) Wenzel, R. N. *Ind. Eng. Chem.* **1936**, *28*, 988.
(26) Cassie, A. B. D.; Baxter, S. *Trans. Faraday Soc.* **1944**, *40* 0546.
(27) Miwa, M.; Nakajima, A.; Fujishima, A. *Langmuir* **2000**, *16* 5754.
(28) Takahara, Y.; Kondo, J. N.; Takata, T.; Domen, K. *Chem. Mater.* **2001**, *13*, 1194.
(29) Seki, K.; Tachiya, M. *J. Phys. Chem. B* **2004**, *108*, 4806.
(30) Chen, X.; Burda, C. *J. Phys. Chem. B* **2004**, *108*, 15446.
(31) http://www.srim.org/.
(32) Zubkov, T.; Stahl, D.; Thompson, T. L.; Pananyotov, D.; Diwald, O.; Yates, J. T. *J. Phys. Chem. B* **2005**, *109*, 15454.
(33) Nakamura, R.; Tanaka, T.; Nakato, Y. *J. Phys. Chem. B* **2004**, *108*, 10617.
(34) Irie, H.; Washizuka, S.; Watanabe, Y.; Kako, T.; Hashimoto, K. *J. Electrochem. Soc.* **2005**, *152*, E351.
(35) Carp, O.; Huisman, C. L.; Reller, A. *Prog. Solid State Chem.* **2004**, *32*, 33.
(36) Bak, T.; Nowotny, J.; Rekas, M.; Sorrell, C. C. *Int. J. Hydrogen Energy* **2002**, *27*, 991.

JP805708W